THE JOURNAL OF PHYSICAL CHEMISTRY C
A JOURNAL OF THE AMERICAN CHEMICAL SOCIETY

pubs.acs.org/JPCC

Article

Illumination Power-Dependent Electroabsorption of Excitons in a $CH_3NH_3PbI_3$ Perovskite Film

Shailesh Rana, Kamlesh Awasthi, Eric Wei-Guang Diau,* and Nobuhiro Ohta*

Cite This: *J. Phys. Chem. C* 2021, 125, 27631−27637

Read Online

ACCESS | Metrics & More | Article Recommendations | Supporting Information

ABSTRACT: Electroabsorption (E-A) spectra of methylammonium lead triiodide ($MAPbI_3$) are found to depend on the power density of the illumination light (IL-D) in both tetragonal and orthorhombic phases when the modulation frequency (M-F) of the applied electric field (***F***) is low. As IL-D increased, the E-A intensity decreased and the shape of the E-A spectra altered from that similar to the second derivative of the exciton absorption band having a Gaussian profile to the one similar to the first derivative, when the M-F of ***F*** is low. When the M-F of ***F*** is high, E-A spectra were independent of the power density of illumination. Orientational polarization of excitons is considered to be induced by ***F*** having a low M-F with strong photoirradiation, following ion migration of MA^+ and I^- along the applied field direction enhanced by photoirradiation.

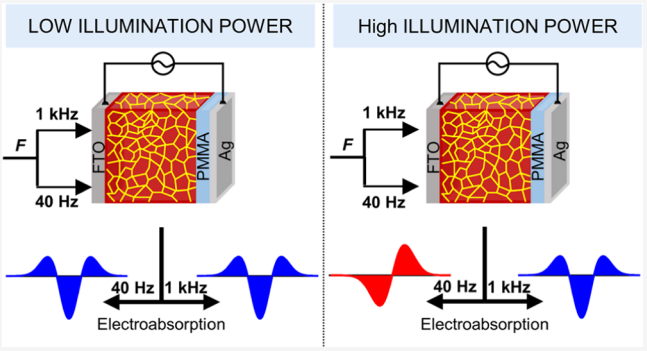

1. INTRODUCTION

Organic−inorganic lead-halide perovskites, especially methylammonium lead triiodide ($MAPbI_3$), have emerged as promising candidates for cheap and abundant energy-consumption materials for next-generation solar cells.[1−6] In devices based on $MAPbI_3$ such as photovoltaic (PV) cells, the excitons produced on absorption play a vital role in dissociating into supply free carriers; it is hence important to understand how an exciton behaves under external stimuli, such as temperature change, photoirradiation, or application of an external electric field.[7−9] Because it has a large relative permittivity, $MAPbI_3$ was expected to have a non-excitonic character, but a clear excitonic nature has been reported in electroabsorption (E-A) spectra.[10−14]

E-A spectra of a $MAPbI_3$ film having a vertical device structure as fluorine-doped tin-oxide (FTO)/$MAPbI_3$/poly(methyl methacrylate) (PMMA)/Al were measured with modulation frequency 40 Hz at varied temperatures, as reported previously.[14] The E-A spectra were essentially independent of the modulation frequency of the applied electric field in the region 40 Hz to 1 kHz; the observed E-A spectra were analyzed with an integral method on assuming that the E-A signal originated from the Stark effect of the exciton absorption band. The binding energy of the exciton and the change in electric dipole moment and polarizability following absorption into the exciton band were also determined. Many groups reported ion migration of I^- and MA^+ ions in darkness, under illumination and on application of an electric field.[15−18] The MA^+ cation at the center of a lead-iodide cage is highly rotationally mobile; photoinduced carriers were suggested to modify the equilibrium of the local unit cell, assisted by a MA^+ rotation.[19] E-A spectra of which the signal intensities depended on the modulation frequency of an applied electric field were also reported by Wu et al.[11] Despite many reports about the mobile characteristics of $MAPbI_3$ in a solid film, our E-A spectra of $MAPbI_3$ film were independent of the modulation frequency of an applied electric field and were analyzed on assuming an immobile and isotropically distributed system.[13,14] At that time, we noticed that our E-A spectra of a $MAPbI_3$ film differed markedly from those reported by Wu et al.[11] This discrepancy has subsequently been resolved because we have found that the E-A spectra depend on the power density of the incident light when the modulation frequency of the applied electric field is low. Hereafter, the power density of illumination, applied electric field, and its modulation frequency are denoted as IL-D, ***F***, and M-F, respectively. Not only the E-A intensity but also the shape of the E-A spectra depended on the IL-D, indicating that a $MAPbI_3$ film under application with ***F*** having low M-F must be regarded as a mobile system only when IL-D is large. When IL-D is small, the E-A spectra observed with a low M-F of ***F*** are essentially the same as those observed with a high M-F. When

Received: July 9, 2021
Revised: November 22, 2021
Published: December 11, 2021

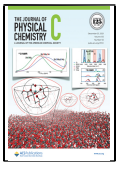

https://doi.org/10.1021/acs.jpcc.1c06129
J. Phys. Chem. C 2021, 125, 27631−27637

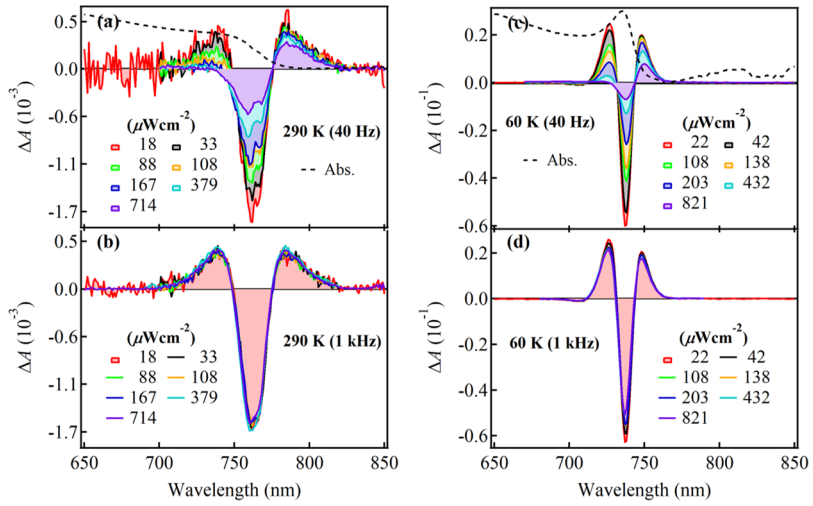

Figure 1. E-A spectra of $MAPbI_3$ at 290 (a,b) and 60 K (c,d) under varied power densities of illumination observed with field strength 0.3 MV cm^{-1} and modulation frequencies 40 Hz (a,c) and 1 kHz (b,d). Absorption spectra at 290 and 60 K are shown as dotted black line in (a,c) respectively.

the IL-D is large, in contrast, the E-A spectra depend on the M-F. The results reported in our previous papers correspond to those obtained with a small IL-D, whereas the E-A spectra reported by Wu et al. are regarded as those observed with a large IL-D. We report here E-A spectra of a $MAPbI_3$ film dependent on the IL-D, which depend also on the M-F of ***F***. These results enable us to conclude that orientational polarization of excitons is induced by ***F*** having low M-F with strong photoirradiation, which enhances migration of MA^+ and I^- ions.

2. EXPERIMENTAL SECTION

2.1. Sample Preparation. The $MAPbI_3$ perovskite film was prepared with a solution-processing method. MAI (homemade) and PbI_2 powders mixed in anhydrous dimethyl formamide in molar ratio 1:1 at 45 mass % were stirred for 12 h at 70 °C in a nitrogen-purged glovebox to prepare the $MAPbI_3$ precursor solution. A polycrystalline thin film of $MAPbI_3$ on a FTO coated glass substrate was prepared by spin-coating the mixed precursor solution of $MAPbI_3$ at 5000 rpm for 15 s, incorporating chlorobenzene after 5 s of spinning and annealed at 100 °C for 10 min; the sample changed from transparent to black.

After deposition of a $MAPbI_3$ layer on FTO, a thin PMMA film was spin-coated on top of the $MAPbI_3$ layer as insulator, which also protected the $MAPbI_3$ layer from the external environment (oxygen and moisture). A semi-transparent layer of aluminum (Al) with thickness ∼15 nm was deposited by thermal evaporation on sample substrates having a PMMA film on the perovskite layer. The FTO and Al films served as electrodes to record E-A spectra.[13,14] The field strength was calculated from the applied voltage divided by the distance between electrodes.

2.2. Optical Measurements. All measurements were conducted under vacuum conditions with a cryogenic refrigerating system (Daikin, V202C5LR), equipped with silica optical windows, a temperature controller (Scientific Inst., model 9600-1), and a silicon diode thermometer.[14] All spectra were recorded with a commercially available spectrometer (JASCO, FP-777), and the intensity of transmitted light (T) controlled with neutral density filters. A sinusoidal ac voltage of modulation frequency in a range 40 Hz to 1 kHz was applied from a function generator between two electrodes attached to the sample. The modulated transmitted light intensity (ΔT) was detected with a lock-in amplifier at the second harmonic mode ($2f$). The dc component T was concurrently recorded with a computer. The E-A spectra were derived on plotting the field-induced change of absorption $\Delta A \left(\equiv -\left(\frac{2\sqrt{2}}{\ln 10}\right)\left(\frac{\Delta T(2f)}{T}\right)\right)$ as a function of wavelength or wavenumber.

3. RESULTS AND DISCUSSION

We recorded E-A spectra of $MAPbI_3$ at 290 and 60 K with varied IL-D using varied M-F of ***F***. The results obtained with M-F 40 Hz and 1 kHz with IL-D from ∼20 to ∼800 $\mu W\ cm^{-2}$ are shown in Figure 1. When the M-F was 1 kHz, the E-A spectra were essentially the same as those reported in our previous papers at both 290 and 60 K; the E-A spectra were nearly independent of the IL-D, as Figure 1 shows. When the M-F was as low as 40 Hz, the E-A spectra observed with IL-D ∼20 $\mu W\ cm^{-2}$ were almost the same as those observed with M-F 1 kHz at both 290 and 60 K, but the E-A signal intensity depended significantly on the IL-D (see Figure 1). As Figure 2 shows, the magnitude of the E-A signal monitored at the minimum of the E-A spectra, that is, 762 nm at 290 K and 738 nm at 60 K, gradually decreased and approached a saturated value with increasing IL-D at M-F 40 Hz. The extended view of the E-A spectra shown in Figure 3 demonstrates that the shape of the E-A spectra observed with M-F 40 Hz also depends on the IL-D at both 290 and 60 K. The E-A spectra observed at 110 K also showed a remarkable IL-D dependence (see Supporting Information, Figure S1) under a M-F 40 Hz, which is similar to the spectra at 290 and 60 K. Note that a $MAPbI_3$ film at 110 K shows the orthorhombic phase, as also the case at 60 K.[14] It should be noted that the IL-D dependence is reversible. Once the magnitude of IL-D is returned to the original one, E-A spectra which are essentially the same as the original one were obtained.

To examine the dependence of the E-A spectra of $MAPbI_3$ on the M-F, we recorded ΔA with two values of IL-D and varied M-F at 290 and 60 K. As shown in Figure 4, $\Delta T/T$, that

https://doi.org/10.1021/acs.jpcc.1c06129
J. Phys. Chem. C 2021, 125, 27631−27637

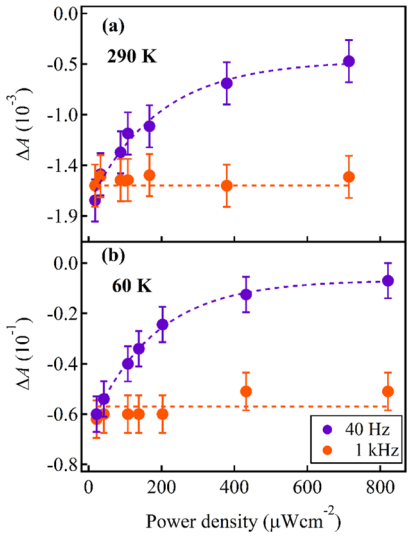

Figure 2. Plots of E-A signal intensity as a function of power density of illumination at 290 K (a) and 60 K (b). The intensity was monitored at the minimum of the E-A spectrum, i.e., 762 nm at 290 K and 738 nm at 60 K. E-A signals measured at modulation frequency 40 Hz and 1 kHz are shown as purple and orange circle, respectively. Broken lines are just for visual guidance.

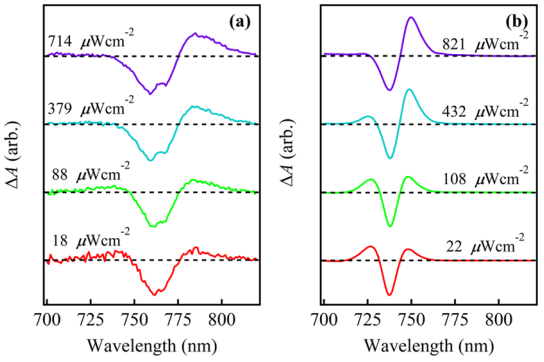

Figure 3. Normalized E-A spectra observed at 290 (a) and 60 K (b) with a modulation frequency of 40 Hz and different illumination power densities, to clearly show the illumination power dependence of the spectral shape of the E-A spectra. These spectra are the same as the ones in Figure 1.

is, ΔA was independent of M-F when IL-D was as small as ∼5 μW cm^{-2}. When IL-D was as large as ∼200 μW cm^{-2}, on the other hand, the magnitude of $\Delta T/T$, which was small with a low M-F, increased monotonically with increasing M-F and nearly saturated about 500 Hz, indicating a slow process that occurs in a millisecond time range is involved in the IL-D dependence of E-A spectra. The M-F dependence was thus observed only with a large IL-D. Figure 4 also shows that the value of the M-F required for the saturation of $\Delta T/T$ is larger at 60 K than at 290 K.

In our previous papers,[13,14] we showed ΔA of a $MAPbI_3$ film to be proportional to the square of the applied field strength. At that time, we paid little attention to the dependence on IL-D; the dependence on applied field strength was thus again measured at 290 and 60 K with IL-D ∼5 and ∼200 μW cm^{-2}, on monitoring ΔA at the minimum of the E-A spectra. As shown in the Supporting Information (Figure S2), ΔA is proportional to the square of the strength of F, regardless of the temperature or IL-D, indicating that the observed E-A

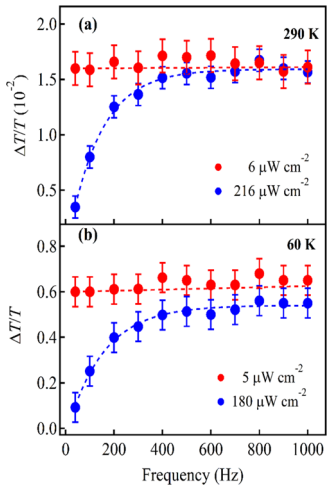

Figure 4. Plots of the field-induced change in transmitted light intensity relative to the transmitted light intensity ($\Delta T/T$) as a function of modulation frequency of applied electric field under two power densities, i.e., 6 and 216 μW cm^{-2} at 290 K (a) 5 and 180 μW cm^{-2} at 60 K (b). The E-A signal was monitored at 762 nm at 290 K and at 738 nm at 60 K, at which E-A spectra show a minimum, with applied field strength 0.3 MV cm^{-1}. Broken lines are just for visual guidance.

spectra of a $MAPbI_3$ film originated from the Stark effect, independent of IL-D or the M-F of F. Note that our previous experiments were undertaken with a small IL-D.

In direct band-gap semiconductors and insulators where weakly bound Wannier excitons are characterized, E-A spectra were shown to be simulated by exciton theory, that is, with physical parameters of binding energy of exciton, thermal broadening factor, and electron-optical parameter including band-gap energy.[20] The major effect of the electric field is considered to cause the bound levels giving exciton bands to be mixed and broadened into a continuum levels. Also, the 1s level is considered to be shifted to lower energy. In the results, the first exciton absorption peak shows a red shift in the presence of electric field, and the oscillation of the absorption profile of the continuum band is expected to be observed above the edge.

According to the exciton theory reported by Blossey,[20] Wannier excitons show the E-A profile such as the one shown in Figure 5, which is quite similar to the ones of the present E-A spectra of $MAPbI_3$ observed with high M-F of F or low M-F of F and small IL-D, and the following characteristics have been pointed out: (1) ΔH_3 should be greater than ΔH_1 except for the case of both small field ($F/F_I < 0.3$) and small broadenings ($\Gamma/R < 0.2$), where F_I, Γ, and R represent

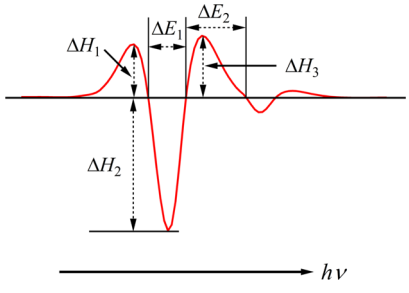

Figure 5. E-A spectra expected in Wannier exciton.

https://doi.org/10.1021/acs.jpcc.1c06129
J. Phys. Chem. C 2021, 125, 27631−27637

ionization field, temperature-dependent broadening parameter, and exciton binding energy, respectively; (2) ΔH_1 and ΔH_3 can increase or decrease with field, whereas ΔH_2 should always increase with field; (3) for large fields, ΔH_2 should approach a constant value, if the exciton is not thermally considered; (4) the first negative oscillation is pinned at $h\nu = E_g - R$, where $h\nu$ and E_g are excitation photon energy and energy gap of semiconductor, respectively; (5) the width ΔE_1 increases slower than $(F/F_I)^{2/3}$ and is temperature dependent, whereas the width ΔE_2 increases as $(F/F_I)^{2/3}$ and is largely temperature independent. Further, the total oscillator strength is considered to be conserved.

When the E-A spectra of $MAPbI_3$ observed in the present study are compared with the ones expected in the exciton model by Blossey,[20] clear differences are noticed. For example, (1) in E-A spectra at a high temperature 290 K, that is, with a large Γ, ΔH_3 is smaller than ΔH_1 (see Figure 3, and Figure 4 of ref 14), in contrast with the theoretical expectation, though ΔH_3 is larger than in ΔH_1 at low temperatures; (2) the magnitude of the E-A signal is proportional to the square of the applied field strength at any monitoring wavelength, as previously reported,[14] indicating that the ratio $\Delta H_1/\Delta H_2/\Delta H_3$ is independent of the magnitude of F; (3) ΔE_1 and ΔE_2 are independent of the magnitude of F, in contrast with the theoretical expectation, and the shape of the E-A spectra is independent of the applied field strength (see Figure 4 of ref 14). Further, total absorption intensity of $MAPbI_3$ solid film changes in the presence of applied electric field, as mentioned later, while the total oscillator strength is considered to be conserved in the theoretical treatment. Regarding the temperature dependence of the E-A spectra, a comparison cannot be carried out in a $MAPbI_3$ solid film because the crystal structure changes with different temperatures and phase transition occurs. Thus, the E-A spectra observed in the present study cannot be reproduced by the simulation given by Blossey.[20] It may be necessary to examine carefully whether optical properties of organic−inorganic perovskites such as $MAPbI_3$, where MA rotation as well as ion migration of MA^+ and I^- ions occurs, are completely similar to the ones of excitons in semiconductor crystals from group IV of the periodic table.

To present the detailed shape of the E-A spectra observed with different IL-Ds, the following equation was used for simulation

$$\Delta A = (fF)^2\left[A_0 A(\nu) + A_1\nu\,\frac{\mathrm{d}}{\mathrm{d}\nu}\left(\frac{A(\nu)}{\nu}\right) + A_2\,\frac{\mathrm{d}^2}{\mathrm{d}\nu^2}\left(\frac{A(\nu)}{\nu}\right)\right] \quad (1)$$

in which F is the magnitude of the electric field, that is, $F = |\boldsymbol{F}|$, f is the internal field factor and A_0, A_1 and A_2 are coefficients. Usually, eq 1 is used for random ensembles of molecules by assuming an isotropic angular distribution of the absorbers,[21−23] and it may be important to note that this equation is applicable not only to spatial fixed molecules (materials) but also to molecules like being able to reorient freely under applied electric field.[21,23] For example, E-A spectra of organic dipolar molecules both in solution and in solid film, which give different spectral shapes of E-A spectra, could be analyzed with eq 1.[24] The simulation of the observed E-A spectra of $MAPbI_3$ film based on this equation may suggest what causes the field-induced change in profile of the E-A spectra.

All the E-A spectra could be reproduced quite well with eq 1 by assuming that only the exciton band having a Gaussian profile shows an electric field effect. Simulation of the E-A spectra at 290 and 60 K observed with M-F 40 Hz and IL-D ~20 or ~800 μW cm^{-2} appear in Figure 6, in which the

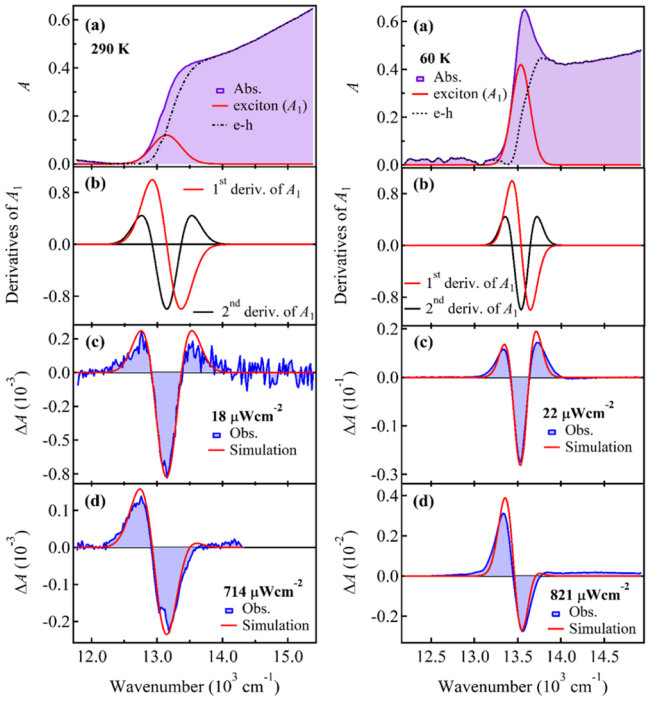

Figure 6. Analysis of E-A spectra of $MAPbI_3$ observed at 290 K (left) and 60 K (right). (a) Absorption spectrum and its decomposition into an exciton band of Gaussian shape (red line) and a continuum band (black dotted line), (b) first derivative (red line) and second derivative (black line) of the exciton absorption band, (c) E-A spectrum observed with small power density of illumination and the simulated spectrum, and (d) E-A spectrum observed with large power density of illumination and the simulated spectrum. The illumination power density used for the E-A measurements is shown in the figure.

absorption spectrum, composed of exciton and continuum bands, and the first and second derivatives of the exciton band are also shown. Simulations of other E-A spectra observed with M-F 40 Hz and varied IL-D are shown in Supporting Information (Figures S3 and S4). Each value of coefficients A_0, A_1 and A_2 at 290 and 60 K used to simulate the E-A spectra observed with M-F 40 Hz and varied IL-D is listed in Supporting Information, Tables S1 and S2. Plots of coefficients A_1 and A_2 as a function of IL-D at 290 and 60 K are shown in Figure 7. With M-F 40 Hz, coefficient A_2 as well as the total intensity of the E-A spectra decreased monotonically with increasing IL-D at both 290 and 60 K, whereas coefficient A_1 monotonically increased with increasing IL-D. Coefficients A_1 and A_2 used to simulate the E-A spectra observed with M-F 1 kHz are essentially the same as those estimated for the E-A spectra observed with IL-D ~20 μW cm^{-2} and M-F 40 Hz.

When the M-F of F is as low as 40 Hz, the shape of the E-A spectra altered from that similar to the second derivative of the exciton absorption band having a Gaussian profile to a shape similar to the first derivative of the exciton band, as the IL-D increased (see Figure 6c,d). Even with varied IL-D, the observed E-A spectra could be reproduced by using eq 1,

https://doi.org/10.1021/acs.jpcc.1c06129
J. Phys. Chem. C 2021, 125, 27631−27637

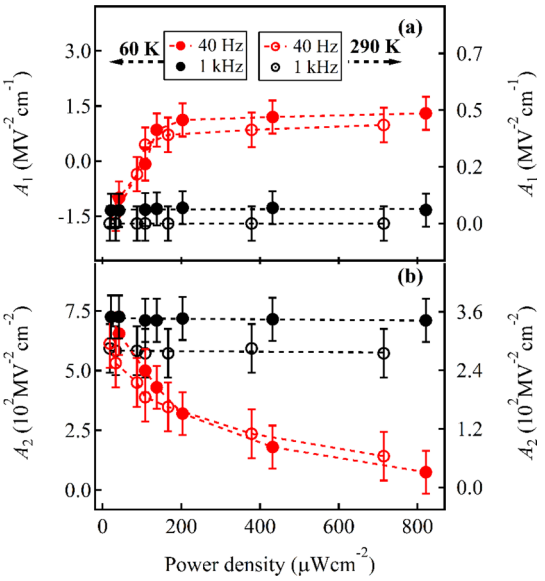

Figure 7. Plots of coefficients A_1 (a) and A_2 (b) used to simulate E-A spectra at 290 K (scale on the right) and 60 K (scale on the left) with eq 1 as a function of power density of illumination (IL-D). The data for the E-A spectra observed with modulation frequencies 40 Hz and 1 kHz are shown with red and black circles, respectively. Broken lines are just for visual guidance.

although the contribution of each derivative component depended on IL-D.

In random ensemble of molecules, where eq 1 is applied in the presence of external electric field, the first term indicates the field-induced change in absorption intensity, and the second and third terms corresponds to the spectral shift and spectral broadening, respectively. With the simulation of the E-A spectra with eq 1, it is noticed that the coefficient A_1 is negligibly small at room temperature, indicating that the Stark effect resulting from the spectral shift of the exciton absorption band is negligible. The fact that no redshift caused by the change in polarizability following absorption is negligible at room temperature is very different from the theory of the electric field effect on absorption spectra of the Wannier exciton.

In random ensemble of molecules, whose E-A spectra are given in eq 1, orientational polarization of electric dipole moment (permanent and/or field-induced dipole) toward the applied electric field direction leads to the enhancement of the first derivative term, that is, increase of A_1 in eq 1. The present results remind such orientational polarization of a dipole. In case of $MAPbI_3$ films, two cases may be able to be considered as the origin of orientational polarization of excitons. One is the reorientation of MA^+ cation, which has an electric dipole moment ~2.3 D,[25] along the applied field direction, and another is an orientation of a pair of MA^+ and I^- ions, which migrate along the applied field direction. Both may induce the orientation of excitons along the applied field direction. It has been reported that photoirradiation greatly reduced the ion migration energy barrier in polycrystalline and single crystalline organic−inorganic halide perovskite materials including $MAPbI_3$.[16] Therefore, orientational polarization of excitons which enhances the A_1 value may be attributed to the ion migration of MA^+ and I^- ions toward the opposite directions to each other in the presence of electric field, because A_1 is strongly enhanced by photoirradiation.

The fact that the total intensity of the E-A signal as well as coefficient A_2 decreased with small M-F and with increasing IL-D indicates a possibility that the electric field applied to a material decreases with increasing IL-D in the presence of $\boldsymbol{F}$ having a low M-F. By a field-induced migration of MA^+ and I^- ions, which produces internal field, the applied field may be screened, resulting in the decrease of the actual applied electric field. This assumption is also reasonable because the field-induced enhancement of A_1 is attributed to the field-induced ion migration of MA^+ and I^- ions which is strongly enhanced by photoirradiation.

It was reported that the line-shape of the E-A spectra could be modified by the field inhomogeneity,[26,27] suggesting that field non-uniformity inside the device due to the drift/diffusion of mobile ions can distort the shape of the E-A spectra. As an example of the experimental evidence of such behavior, the electric field effects on absorption (reflection) spectra of germanium solid was pointed out. It is well known that the shape of the E-A spectra of germanium solid depends remarkably on the applied field strength,[28,29] and so it is easily expected that the spectral shape of E-A spectra of germanium is affected by field inhomogeneity. In the present case of $MAPbI_3$, on the other hand, the spectral shape of the E-A spectra is independent of the applied field strength, as already mentioned. Even when non-uniformity of the field exists inside the sample, therefore, the change in spectral shape cannot be expected in the E-A spectra of $MAPbI_3$, though the magnitude of the E-A signal may be affected by the field inhomogeneity. Therefore, it is unlikely that the change in spectral shape of E-A spectra of $MAPbI_3$ in the present study observed with different photoirradiation intensities results from the field inhomogeneity.

Wu et al. analyzed E-A spectra of $MAPbI_3$ on assuming a second-derivative line shape of the absorption spectrum.[11] The magnitude of $|\Delta\mu|$ was reported to decrease with increasing M-F of $\boldsymbol{F}$. Their analysis is unacceptable because the E-A spectra were measured at frequency 91 Hz and light intensity 2 mW cm^{-2}, which is greater than the largest IL-D in the present experiments. The E-A spectra reported by Wu et al. resemble those obtained in our present experiments with a large IL-D, that is, similar to the first-derivative line shape of the exciton absorption band. Those authors also reported the relative permittivity (ε), measured with electrochemical impedance spectra under the illumination conditions, as a function of frequency, such that ε increased with decreasing frequency. Juarez-Perez et al.[19] also reported that a large relative permittivity was induced under 1 sun illumination in $MAPbX_3$ perovskite including $MAPbI_3$, especially at small frequencies. There is thus no doubt that ε of a $MAPbI_3$ film at low frequency increases with intense illumination. The monotonic decrease of the total E-A signal intensity as well as the coefficient A_2 with increasing IL-D at 40 Hz, shown in Figures 2 and 7, can then be attributed to a photoinduced decrease of electric field applied to the $MAPbI_3$ film caused by an increase of ε. The strength of an electric field in a dielectric is decreased by factor $1/\varepsilon$ relative to vacuum.[30] The increase of ε with a large IL-D under an application of $\boldsymbol{F}$ with a low M-F occurs probably through the field-induced ion migration of MA^+ and I^- ions. Only when the M-F of $\boldsymbol{F}$ is less than 500 Hz, ε is considered to depend remarkably on the IL-D, as shown in Figure 4.

As shown in Figure 7 and Tables S1 and S2 of Supporting Information, coefficient A_2 decreased to ~22 and 11% of the

https://doi.org/10.1021/acs.jpcc.1c06129
J. Phys. Chem. C 2021, 125, 27631−27637

initial values, when the IL-D increased from ∼20 to ∼800 μW cm^{-2} at 290 and 60 K, respectively. If these decreases originated from an increased ε of the $MAPbI_3$, ε would increase by factor ∼2.1 or ∼3.0 with increasing IL-D (see Table S3 of Supporting Information). Note that the E-A signal is proportional to the square of the strength of the applied field. ε of $MAPbI_3$ films estimated by Wu et al. with IL-D 2 mW cm^{-2} is ∼300 at 100 Hz and ∼90 at 1 kHz. The ratio of these two, that is, 300/90 = 3.3, is roughly the same as the above-mentioned ratio. E-A spectra recorded with M-F 1 kHz are independent of IL-D and are essentially the same as that obtained with a small IL-D and low M-F of $\boldsymbol{F}$ (see Figures 1 and 2).

Coefficients A_0 and A_1 are also affected by a change in ε, that is, by a change in field strength, which depends on IL-D. On assuming that the dependence of coefficient A_2 on IL-D results from the varied field strength, coefficients A_0 and A_1 evaluated from the simulation of the E-A spectra obtained with M-F 40 Hz became modified so that these were obtained under the same field strength. The values were normalized to those obtained with the smallest IL-D. Plots of modified A_0 and A_1 as a function of IL-D are shown in Supporting Information (Figure S5). Both A_0 and A_1 show a monotonic change with increasing IL-D. As already mentioned, the increase of coefficient A_1 with increasing IL-D is attributed to the orientational polarization of excitons, which probably results from a migration of a pair of ions MA^+ and I^- enhanced by photoirradiation to the opposite direction along the applied field direction.

Usually, the incident photon to current conversion efficiency in solar cells is measured with 1 sun (100 mW cm^{-2}). The magnitude of IL-D used in the present study, for example, 20 or 800 μW cm^{-2} corresponds to 0.0002 and 0.008 sun, respectively, which are much weaker than the illumination light condition of 1 sun. According to the present IL-D dependence of E-A spectra, sample condition of $MAPbI_3$ film under light illumination with 1 sun may be similar to that with the high IL-D such as 800 μW cm^{-2} in the present experiment, where migration of MA^+ and I^- ions is enhanced by photoirradiation. Then, it is interesting to know how the incident photon to current efficiency of solar cell of $MAPbI_3$ is related to the illumination light density. This is very important to consider the PV devices with dim irradiation, for example, for indoor PV application. This will be a future problem.

As we reported for a silver iodide crystal[31,32] and as reported for $MAPbI_3$ crystal,[33] ionic conductivity can be altered by photoirradiation. Then, it is also interesting to know how the present illumination power dependence of E-A spectra is related to illumination power dependence of ionic conductivity of $MAPbI_3$ film, which will be also examined as a future work.

4. CONCLUSIONS

E-A spectra of $MAPbI_3$ perovskite film were recorded with various intensities for absorption light and with different modulation frequencies of applied electric field ($\boldsymbol{F}$). Then, it is found that E-A spectra observed at a small modulation frequency of $\boldsymbol{F}$ depend on the IL-D; the intensity of the E-A signal decreased with increasing IL-D, and the shape of the E-A spectra changed from that similar to the second derivative to that of the first derivative of the exciton absorption band having a Gaussian profile, as IL-D increased. When the modulation frequency of $\boldsymbol{F}$ was high, for example, 1 kHz, E-A spectra were independent of IL-D. The shape of the E-A spectra was different from the one theoretically expected for the Wannier exciton. Then, the observed E-A spectra were simulated by a linear combination of the zeroth, first and second derivative shapes of the exciton absorption band having a Gaussian profile, which is usually used for random ensemble molecules, and well reproduced. The dependence of E-A spectra on the IL-D results from the relative permittivity (ε) of a $MAPbI_3$ film being dependent on the IL-D; under an application of $\boldsymbol{F}$ of low modulation frequency, ε increases with increasing IL-D, leading to a monotonic decrease of the effective electric field applied to a $MAPbI_3$ film. This is attributed to ion migration of MA^+ and I^- ions along the applied field direction, which produces an internal electric field and reduces the applied field. The change in the shape of the E-A spectra with increasing IL-D is attributed to orientational polarization of excitons induced by applied electric field, which probably results from a migration of ion pairs of MA^+ and I^-, that is, the ion migration and orientational polarization of excitons along the applied electric field is enhanced by strong photoirradiation.

■ ASSOCIATED CONTENT

Supporting Information

The Supporting Information is available free of charge at https://pubs.acs.org/doi/10.1021/acs.jpcc.1c06129.

Power-dependent E-A spectra at 110 K, field-strength dependence of E-A signal at 290 and 60 K, simulation of power-dependent E-A spectra at 290 and 60 K, IL-D dependence of corrected coefficients A_0 and A_1, fitted parameters to reproduce the E-A spectra at 290 and 60 K, and increment factor in ε derived from the A_1 value determined at high and low IL-D (PDF)

■ AUTHOR INFORMATION

Corresponding Authors

Eric Wei-Guang Diau − *Department of Applied Chemistry and Institute of Molecular Science and Center for Emergent Functional Matter Science, National Yang Ming Chiao Tung University, Hsinchu 300093, Taiwan;* orcid.org/0000-0001-6113-5679; Email: diau@mail.nctu.edu.tw

Nobuhiro Ohta − *Department of Applied Chemistry and Institute of Molecular Science and Center for Emergent Functional Matter Science, National Yang Ming Chiao Tung University, Hsinchu 300093, Taiwan;* orcid.org/0000-0003-4255-6448; Email: nohta@nctu.edu.tw

Authors

Shailesh Rana − *Department of Applied Chemistry and Institute of Molecular Science, National Yang Ming Chiao Tung University, Hsinchu 300093, Taiwan*

Kamlesh Awasthi − *Department of Applied Chemistry and Institute of Molecular Science and Center for Emergent Functional Matter Science, National Yang Ming Chiao Tung University, Hsinchu 300093, Taiwan;* orcid.org/0000-0001-7852-059X

Complete contact information is available at: https://pubs.acs.org/10.1021/acs.jpcc.1c06129

Notes

The authors declare no competing financial interest.

■ ACKNOWLEDGMENTS

Taiwan Ministry of Science and technology (MOST 108-2113-M-009-001 and MOST 109-2123-M-009-001) and Center for Emergent Functional Matter Science of National Yang Ming Chiao Tung University from The Featured Areas Research Center Program within the framework of the Higher Education Sprout Project by Taiwan Ministry of Education (MOE) supported this work.

■ REFERENCES

(1) Li, J.; Dagar, J.; Shargaieva, O.; Flatken, M. A.; Köbler, H.; Fenske, M.; Schultz, C.; Stegemann, B.; Just, J.; Többens, D. M.; et al. 20.8% Slot-Die Coated $MAPbI_3$ Perovskite Solar Cells by Optimal DMSO-Content and Age of 2-ME Based Precursor Inks. *Adv. Energy Mater.* **2021**, *11*, 2003460.

(2) Zhao, L.; Lee, K. M.; Roh, K.; Khan, S. U. Z.; Rand, B. P. Improved Outcoupling Efficiency and Stability of Perovskite Light-Emitting Diodes Using Thin Emitting Layers. *Adv. Mater.* **2019**, *31*, 1805836.

(3) Green, M. A.; Ho-Baillie, A.; Snaith, H. J. The Emergence of Perovskite Solar Cells. *Nat. Photonics* **2014**, *8*, 506−514.

(4) Yoo, E. J.; Lyu, M.; Yun, J.-H.; Kang, C. J.; Choi, Y. J.; Wang, L. Resistive Switching Behavior in Organic-Inorganic Hybrid $CH_3NH_3PbI_{3-x}Cl_x$ Perovskite for Resistive Random Access Memory Devices. *Adv. Mater.* **2015**, *27*, 6170−6175.

(5) Hu, X.; Zhang, X.; Liang, L.; Bao, J.; Li, S.; Yang, W.; Xie, Y. High-Performance Flexible Broadband Photodetector Based on Organolead Halide Perovskite. *Adv. Funct. Mater.* **2014**, *24*, 7373−7380.

(6) Jena, A. K.; Kulkarni, A.; Miyasaka, T. Halide Perovskite Photovoltaics: Background, Status, and Future Prospects. *Chem. Rev.* **2019**, *119*, 3036−3103.

(7) D'Innocenzo, V.; Grancini, G.; Alcocer, M. J. P.; Kandada, A. R. S.; Stranks, S. D.; Lee, M. M.; Lanzani, G.; Snaith, H. J.; Petrozza, A. Excitons versus Free Charges in Organo-Lead Tri-Halide Perovskites. *Nat. Commun.* **2014**, *5*, 3586.

(8) Kundu, S.; Kelly, T. L. In Situ Studies of the Degradation Mechanisms of Perovskite Solar Cells. *EcoMat* **2020**, *2*, No. e12025.

(9) Xiao, Z.; Yuan, Y.; Shao, Y.; Wang, Q.; Dong, Q.; Bi, C.; Sharma, P.; Gruverman, A.; Huang, J. Giant Switchable Photovoltaic Effect in Organometal Trihalide Perovskite Devices. *Nat. Mater.* **2015**, *14*, 193−198.

(10) Hu, M.; Bi, C.; Yuan, Y.; Xiao, Z.; Dong, Q.; Shao, Y.; Huang, J. Distinct Exciton Dissociation Behavior of Organolead Trihalide Perovskite and Excitonic Semiconductors Studied in the Same System. *Small* **2015**, *11*, 2164−2169.

(11) Wu, X.; Yu, H.; Li, L.; Wang, F.; Xu, H.; Zhao, N. Composition-Dependent Light-Induced Dipole Moment Change in Organometal Halide Perovskites. *J. Phys. Chem. C* **2015**, *119*, 1253−1259.

(12) Ziffer, M. E.; Mohammed, J. C.; Ginger, D. S. Electroabsorption Spectroscopy Measurements of the Exciton Binding Energy, Electron-Hole Reduced Effective Mass, and Band Gap in the Perovskite $CH_3NH_3PbI_3$. *ACS Photonics* **2016**, *3*, 1060−1068.

(13) Awasthi, K.; Du, K.-B.; Wang, C.-Y.; Tsai, C.-L.; Hamada, M.; Narra, S.; Diau, E. W.-G.; Ohta, N. Electroabsorption Studies of Multicolored Lead Halide Perovskite Nanocrystalline Solid Films. *ACS Photonics* **2018**, *5*, 2408−2417.

(14) Hamada, M.; Rana, S.; Jokar, E.; Awasthi, K.; Diau, E. W.-G.; Ohta, N. Temperature-Dependent Electroabsorption Spectra and Exciton Binding Energy in a Perovskite $CH_3NH_3PbI_3$ Nanocrystalline Film. *ACS Appl. Energy Mater.* **2020**, *3*, 11830−11840.

(15) Futscher, M. H.; Lee, J. M.; McGovern, L.; Muscarella, L. A.; Wang, T.; Haider, M. I.; Fakharuddin, A.; Schmidt-Mende, L.; Ehrler, B. Quantification of Ion Migration in $CH_3NH_3PbI_3$ Perovskite Solar Cells by Transient Capacitance Measurements. *Mater. Horiz.* **2019**, *6*, 1497−1503.

(16) Xing, J.; Wang, Q.; Dong, Q.; Yuan, Y.; Fang, Y.; Huang, J. Ultrafast Ion Migration in Hybrid Perovskite Polycrystalline Thin Films under Light and Suppression in Single Crystals. *Phys. Chem. Chem. Phys.* **2016**, *18*, 30484−30490.

(17) Zhao, Y.-C.; Zhou, W.-K.; Zhou, X.; Liu, K.-H.; Yu, D.-P.; Zhao, Q. Quantification of Light-Enhanced Ionic Transport in Lead Iodide Perovskite Thin Films and Its Solar Cell Applications. *Light: Sci. Appl.* **2017**, *6*, No. e16243.

(18) Yun, J. S.; Seidel, J.; Kim, J.; Soufiani, A. M.; Huang, S.; Lau, J.; Jeon, N. J.; Seok, S. I.; Green, M. A.; Ho-Baillie, A. Critical Role of Grain Boundaries for Ion Migration in Formamidinium and Methylammonium Lead Halide Perovskite Solar Cells. *Adv. Energy Mater.* **2016**, *6*, 1600330.

(19) Juarez-Perez, E. J.; Sanchez, R. S.; Badia, L.; Garcia-Belmonte, G.; Kang, Y. S.; Mora-Sero, I.; Bisquert, J. Photoinduced Giant Dielectric Constant in Lead Halide Perovskite Solar Cells. *J. Phys. Chem. Lett.* **2014**, *5*, 2390−2394.

(20) Blossey, D. F. Wannier Exciton in and Electric Field. II. Electroabsorption in Direct-Band-Gap Solids. *Phys. Rev. B: Solid State* **1971**, *3*, 1382−1391.

(21) Liptay, W. Dipole Moments and Polarizabilities of Molecules in Excited Electronic States. In *Excited States*; Lim, E. C., Ed.; Academic Press: New York, 1974; Vol. *1*, pp 129−229.

(22) Bublitz, G. U.; Boxer, S. G. Stark Spectroscopy: Applications in Chemistry, Biology, and Materials Science. *Annu. Rev. Phys. Chem.* **1997**, *48*, 213−242.

(23) Jalviste, E.; Ohta, N. Theoretical foundation of Electroabsorption Spectroscopy: Self-Contained Derivation of the Basic Equations with the Direction Cosine Method and the Euler Angle Method. *J. Photochem. Photobiol., C* **2007**, *8*, 30−46.

(24) Tayama, J.; Iimori, T.; Ohta, N. Comparative Study of Electroabsorption Spectra of Polar and Non-Polar Organic Molecules in Solution and in a Polymer Film. *J. Chem. Phys.* **2009**, *131*, 244509.

(25) Frost, J. M.; Butler, K. T.; Brivio, F.; Hendon, C. H.; Van Schilfgaarde, M.; Walsh, A. Atomistic Origins of High-Performance in Hybrid Halide Perovskite Solar Cells. *Nano Lett.* **2014**, *14*, 2584−2590.

(26) Evangelisti, F.; Frova, A. Anomalous Franz-Keldysh Effect in the Electroreflectance of Semiconductors. *Solid State Commun.* **1968**, *6*, 621−625.

(27) Aspnes, D. E.; Frova, A. Influence of Spatially Dependent Perturbations on Modulated Reflectance and Absorption of Solids. *Solid State Commun.* **1993**, *88*, 1061−1065.

(28) Hamakawa, Y.; Germano, F. A.; Handler, P. Interband Electro-Optical Properties of Germanium. I. Electroabsorption. *Phys. Rev.* **1968**, *167*, 703−709.

(29) Nishino, T.; Hamakawa, Y. Low Temperature Electro-Reflectance of Germanium in Spectral Region from 0.7 to 2.6 eV. *J. Phys. Soc. Jpn.* **1969**, *26*, 403−412.

(30) Bottcher, C. J. F.; Bordewijk, P. *Theory of Electric Polarization*; Elsevier: Amsterdam, Netherlands, 1978; Vol. *1*.

(31) Khaton, R.; Kashiwagi, S.-i.; Iimori, T.; Ohta, N. Reversible Photoswitching Behavior in Bulk Resistance and in Color of Polycrystalline β-AgI at Room Temperature. *Appl. Phys. Lett.* **2008**, *93*, 234102−234104.

(32) Sabeth, F.; Iimori, T.; Ohta, N. Gigantic Photoresponse and Reversible Photoswitching in the Ionic Conductivity of Polycrystalline β-AgI. *J. Phys. Chem. C* **2012**, *116*, 9209−9213.

(33) Kim, G. Y.; Senocrate, A.; Yang, T.-Y.; Gregori, G.; Grätzel, M.; Maier, J. Large Tunable Photoeffect on Ion Conduction in Halide Perovskites and Implications for Photodecompositions. *Nat. Mater.* **2018**, *17*, 445−449.

https://doi.org/10.1021/acs.jpcc.1c06129
J. Phys. Chem. C 2021, 125, 27631−27637